

Design and Performance Analysis of Liquid Fueled Pulsejet Engine

*Bhogaraju Nikhil, Guglothu Purnivas, B. Veera Brahmendra Rao,
N. Kalyan Chakravarthy, N. Leela Prasad*

Department of Mechanical Engineering, Vignan Institute of Technology & Science. Hyderabad, India

Abstract

Jet engines are big complex contraptions pushing multimillion dollar aircraft through the skies. Pulsejet engine is considered as one of the first ever built jet engine used for airborne propulsion. The idea here is to design, fabricate, and analyze the performance of the scaled down version of the engine with the fuel being Petrol and material being stainless steel (SS). The valveless pulsejet engine represents an attractive alternative to current aerospace propulsion systems. The main advantage of pulsejet engines are their construction simplicity as the engine is essentially a hollow tube with no moving parts. This results in a highly reliable system which is economical to construct and maintain. Research and development of pulsejet engines has been mainly confined to enthusiast circles and small scale aerospace applications, such as UAVs.

In this study a valveless pulsejet engine and its test-stand is designed, fabricated and tested extensively. The design specifies, the engine produced 6kg of thrust and weighs 5.25 kg.

Keywords - *Valveless Pulsejet Engine, Pulsejet Engine, Liquid fuel Pulsejet Engine*

1. Introduction

The valveless Pulsejet engine [1] represents an attractive alternative to current aerospace propulsion systems. The main advantage of pulsejet engine is their construction simplicity as the engine is essentially a hollow tube with no moving parts. This results in a highly reliable system which is economical to construct and maintain. Research and Development of Pulsejet engines have been mainly confined to enthusiast's circles and small scale aerospace applications, such as UAV's.

A pulsejet is a simple form of an air breathing jet engine that has few or no moving parts. The pulsejet acts in cycles, or pulses, where air is drawn into a combustion chamber, mixed with fuel, ignited, and then accelerated out of a nozzle providing thrust. There are two basic categories of a pulsejet engine. The first is a valved design, in which the combustion process is controlled by valves. The air passes through these valves, and then when combustion begins, the valves slam shut, forcing the combustion products to exit through the nozzle, providing forward thrust. This type of engine requires more parts for the valve system, which results in potential for

more problems. The second category of pulsejets is known as a valveless system, in which the valve system is completely removed. This results in the valveless designs having no moving parts, resulting in an engine that is easier to construct and maintain. Valveless pulsejets have three basic parts: the intake tubes, combustion chamber, and exhaust nozzle. When combustion occurs, the intake tubes attempt to limit the expulsion of combustion products, but do not stop it all together, as in the valved design. This means that while the majority of the combustion products exit the nozzle, a small part will exit from the intake. Because of this, many valveless designs have the intake facing in the same direction as the nozzle, to provide all thrust in the same direction. The engine is built out of stainless steel 304 and uses a fuel injection system. The ideal test apparatus consists of thermo couple placed in the combustion chamber, with the purpose of measuring temperature on the pulsejet. In this study a valveless pulsejet engine is designed, fabricated and tested extensively.

1.1. Lenoir Cycle

The Lenoir cycle is an idealized thermodynamic cycle often used to model a pulse jet engine. It is based on the operation of an engine patented by Jean Joseph Etienne Lenoir in 1860. This engine is often thought of as the first commercially produced internal combustion engine. The absence of any compression process in the design leads to lower thermal efficiency than the more well known Otto cycle and Diesel cycle.

The Pressure - Specific Volume & Temperature – Entropy diagrams of Lenoir cycle [2] are shown in Figure 1 and Figure 2 respectively.

- Process 1-2: Constant volume heat addition
- Process 2-3: Isentropic expansion
- Process 3-1: Constant pressure heat rejection

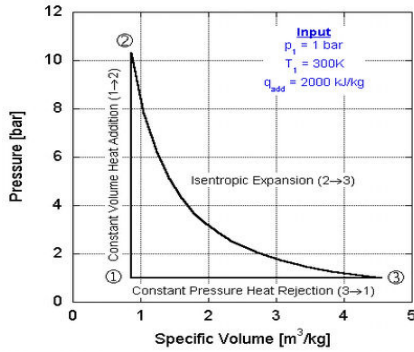


Fig. 1: Lenoir Cycle P-V diagram

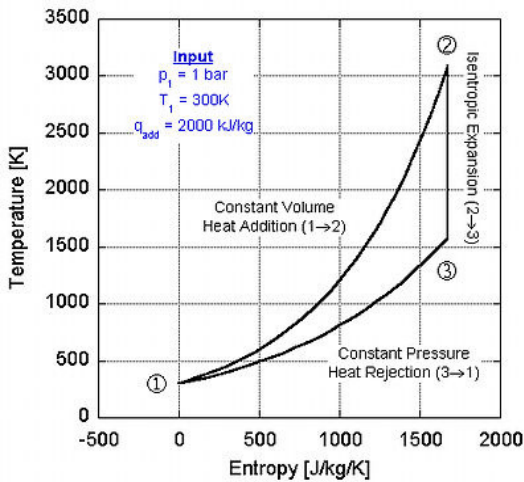


Fig. 2: Lenoir Cycle T-S diagram

1.2. Bernoulli's Equation

The Bernoulli's equation is shown below.

$$\frac{v_1^2}{2} + gh_1 + \frac{p_1}{\rho} = \frac{v_2^2}{2} + gh_2 + \frac{p_2}{\rho} \quad \dots(1)$$

Where, v_1 represents velocity of gas in chamber and is equal to 0 m/s and v_2 represents the velocity at the end of the pipe. Assume height differences (h_1 and h_2) are negligible as $h_1 = h_2$ as this is a frictionless and isentropic process, the Equation 1 reduces to:

$$v_2 = \sqrt{\frac{2}{\rho}(p_1 - p_2)} \quad \dots(2)$$

Since $p_1 > p_2$ and $(p_1 - p_2) > 0$, hence the velocity increases due to the pressure difference between the points. This velocity increase provides the gas in the combustion chamber with inertia. As the exhaust gases move from the combustion chamber to the exhaust, there is a partial vacuum within the chamber; this phenomenon is known as the Kadenacy effect.

2. Design

Main design was initiated by volume of combustion chamber to thrust by an empirical relation. Later, CAD model has been

designed using PTC CREO 2.0. as shown in Figure 3 and Figure 4.

2.1. Volume of combustion chamber

From statistical analysis, Thrust for pulsejet is calculated by using V_{cc} relation.

$$\begin{aligned} \text{Thrust} &= 4453.98V_{cc} + 1.448 \\ 6 &= 4453.98V_{cc} + 1.448 \end{aligned}$$

Therefore, Volume of combustion chamber (V_{cc});

$$V_{cc} = 1.10363 * 10^{-03} \text{ m}^3$$

2.2.. Exhaust Calculations

$$\begin{aligned} \text{Area of exhaust}(A_{EX}) &= 6.12 * 10E -03 \text{ m}^2 \\ \text{Diameter of exhaust}(D_{EX}) &= 3.5 \text{ inch} \end{aligned}$$

2.3. Intake Calculations

From statistical analysis,

$$\begin{aligned} \frac{A_{EX}}{A_{Intake}} &= 4.6 \\ A_{Intake} &= \frac{A_{EX}}{4.6} = \frac{6.12 * 10E - 03}{4.6} = 1.33 * 10E - 03 \\ D_{intake} &= 1.62 \text{ inch} \end{aligned}$$

2.4. Nozzle Design

Using equation (1)

$$\frac{v_1^2}{2} + gh_1 + \frac{p_1}{\rho} = \frac{v_2^2}{2} + gh_2 + \frac{p_2}{\rho}$$

Here

$p_2 = 0.2$ bar (assumption);

$r_{air} = 1.2$ kg/m³;

$r_{petrol} = 737$ kg/m³;

$$r_{mixture} = 737 + (1/15) * 1.2 = 737.07$$

hence $v_2 = 96.2$ m/s

Also $v_2 = v_3$.

$$Q = A_3 v_3$$

$$3.115 * 10E-03 = A_3 * 96.2$$

$$A_3 = 1.97 * 10E-02 \text{ m}^2$$

$$D_3 = 1.88 \text{ inch}$$

By statistical analysis, suitable lengths [5] are determined at each section and final dimensions have been considered.

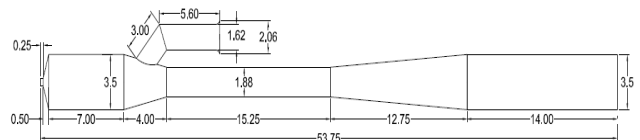


Fig. 3: Pulsejet engine with final dimensions (inches)



Fig. 4: CAD Model designed in PTC CREO 2.0

2.5. Thrust calculation

The thrust is given by,

$$\text{Thrust} = 4453.98V_{cc} + 1.448$$

Thrust at any point within the cycle is given by,

$$F = m_e v_e + m_0 v_0 + (P_e - P_0)A_e$$

The relation between Flow rate \dot{m} & Volume V is given by,

$$\dot{m} = \rho \cdot V \cdot A$$

Where, ρ is density of fuel and A is the cross sectional area of combustion chamber & V is the volume of combustion chamber.

3. Thermal Analysis

Heat supplied, $Q_s = C_v (T_2 - T_1)$ --- (3)

Heat Rejected, $Q_r = C_p (T_3 - T_1)$ --- (4)

$$W = Q_s - Q_r$$

$$h = W/Q_3$$

$$\frac{C_p}{C_v} = 1.4 \text{ (assumption)}$$

$$T_2 = 800^\circ\text{C} = 800 + 273 = 1073\text{K}$$

$$T_1 = 27^\circ\text{C} = 300\text{K}$$

$$\frac{T_2}{T_3} = \left(\frac{p_2}{p_3}\right)^{\frac{\gamma-1}{\gamma}}$$

$$P_2 = 1.5 \text{ bar (after combustion)} \text{ \& } P_3 = 0.2 \text{ bar (assumptions)}$$

$$T_3 = 603.376 \text{ K}$$

$$C_p \text{ (petrol- Gaseous state)} = 2.2 \text{ KJ/KgK [6]}$$

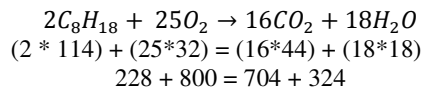
$$C_v \text{ (petrol- Gaseous state)} = 1.57 \text{ KJ/KgK [6]}$$

$$\therefore Q_s = 1213.6 \text{ KJ}$$

$$\therefore Q_r = 667.409 \text{ KJ}$$

$$\text{Efficiency (h)} = 45\%$$

3.1. Air Fuel Ratio



∴ Air required for complete combustion
= 15.25 Kg/Kg of fuel

3.2. Mixture Velocity

MPFI pump pressure – 3.5 bar

Leaf blower discharge = 2.8 m³/min

Leaf blower outlet diameter = 20 mm

$$\dot{Q} = A * V; \text{Equ-3}$$

$$\frac{2.8}{60} = \frac{\pi}{4} (0.02^2) * v$$

$$V_{air} = 148.5 \text{ m/s}$$

Pump flow rate – 200 lt/hr = 3 lt/min = 3 * 10E-03 m³/min

$$\dot{Q} = A * V$$

$$V_{fuel} = 42.44 \text{ m/s}$$

Mixture velocity

$$= \frac{(v_{air} * \text{fuel to air ratio}) + v_{fuel}}{2}$$

$$= 95.47 \text{ m/s}$$

Mass flow rate of mixture

$$\text{Air} = 2.8 \text{ m}^3/\text{min} = 46.6 \text{ Lt/sec} = 3.06 \text{ Kg/sec}$$

$$\text{Fuel} = 200 \text{ Lt/hr} = 0.055 \text{ Kg/sec}$$

Mass flow rate of Air- Fuel mixture:

$$3.06 + 0.055 = 3.115 \text{ Kg/sec}$$

4. Design of Fuel Injector

Our primary design constraint was to attain swirling motion of air-fuel mixture in the combustion chamber with help of fuel injector, as swirling attains more efficient combustion [3-4].

The injector shown in Figure 5 was made out of a stainless steel tube of 1 mm diameter and 1 mm thickness. 6 holes were drilled in total, 3 on right top of central axis, 2 on left bottom of central axis & 1 on bottom central axis. Each hole had a diameter of 0.5 mm and electron discharge machining (EDM) was used to drill.



Fig. 5: Fuel Injector with 6 holes (Right side view)

5. Finite Elemental Analysis

FEA relates to a computer model that has a material or design that is stressed and analyzed for specific results. It is used for refinement of new or existing product design. If there is a structural failure, FEA will help determine the modifications of design to meet the respective requirements. FEA uses a complex system of plotting of points called nodes which makes grid called a mesh. This mesh is programmed to contain the material and structural properties which defines the structure’s reaction to certain loading conditions. Nodes are assigned at a certain density throughout the material depending on the anticipated stress levels of a particular area. Regions which receive large amounts of stress usually have a higher node density than those which experience little or no stress. The mesh acts like a spider web from each node and in that there extends a mesh element to each of the adjacent nodes. The web of vectors carries the material properties of the object, creating many elements [7, 8]. In this project, FEA is carried out on test stand using ANSYS 14.5. The CAD model can be imported as either IGES or STEP format to ANSYS from PTC CREO 2.0. In this case, STEP format is chosen since there will be a minimal amount of data loss.

The test stand was primarily designed to carry the battery and the pulsejet engine.

5.1. Loads acting on Test Stand

Analysis is carried out based on loads shown in table 1.

Table 1. Loads acting on test stand

S.No	Name	Load (Kg)
1	Battery	10
2	Pulsejet engine	5.25

5.2. Structural analysis of Test Stand

The structural analysis was carried out to find out equivalent stress, factor of safety and total deformation of the chassis. The meshed model and the properties are shown in Figure 6 and table 2 respectively. Analytical results of the chassis are shown in Figure 7, Figure 8 and Figure 9.

Table 2. Mesh properties of test stand

Nodes	158585
Elements	28090
Mesh metric	Aspect ratio
Min	1.8654
Max	19.215
Average	5.3579
Standard Deviation	1.9336

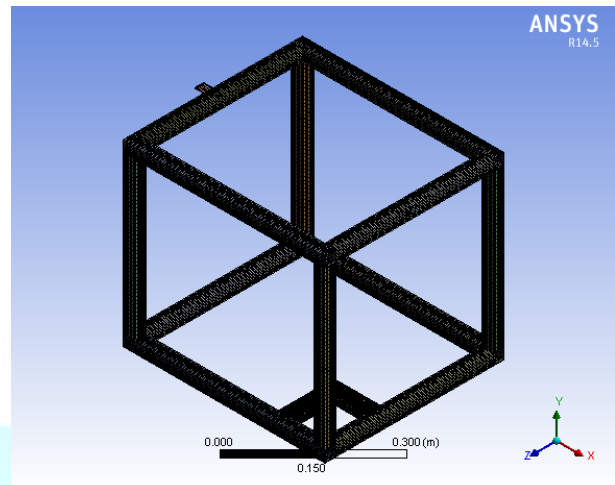


Fig. 6: Meshed model of Test Stand

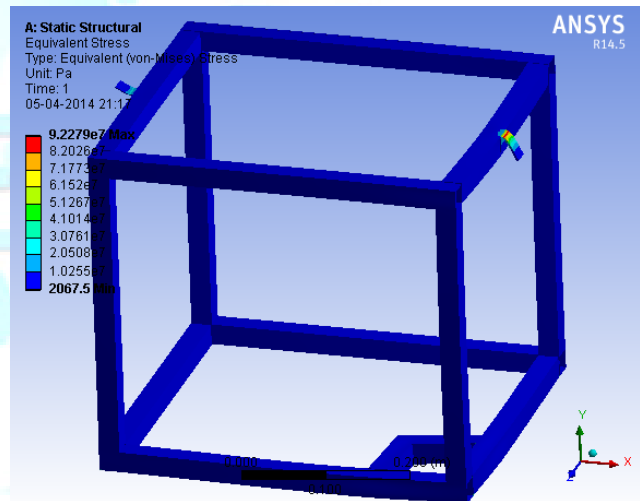


Fig. 7: Equivalent stress analysis of test stand

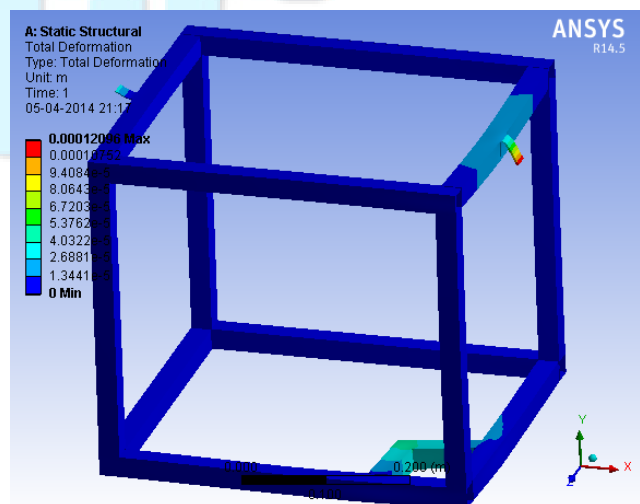


Fig. 8: Total Deformation analysis of test stand

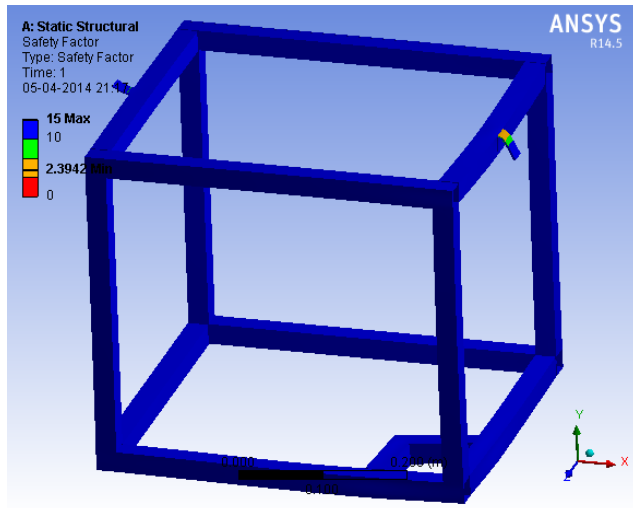


Fig. 9: Safety Factor analysis of test stand

6. Conclusions

Combustion event begins when petrol and air mix and are brought to their auto-ignition temperature through mixing with residual hot products from the previous cycle. The pressure and temperature begin to increase in the combustion chamber. Air continues entering the combustion chamber through the inlet with reduced velocity.

Combustion continues, and peak pressure and temperature are reached in the combustion chamber. Compression waves are generated and propagate into the inlet and the exhaust tube.

Expansion waves are generated at the exhaust duct exit and travel back to the combustion chamber. Pressure decreases in the combustion chamber and the gas velocity out of the inlet and the exit reach their maximum. Most of fuel is burned by this stage.

The combustion chamber pressure decreases below atmospheric pressure, causing air to enter the combustion chamber through the inlet. Hot products continue to be expelled from the exhaust duct.

Cold air from the inlet continually enters the combustion chamber. Hot gas in the exhaust duct is pushed back to the combustion chamber. The pressure in the combustion chamber continues to increase. Backflow continues, but its negative velocity becomes smaller. When the pressure in the combustion chamber approaches atmospheric pressure and air from the inlet mixes with petrol in the combustion chamber, the next cycle begins.

It was observed that chemical reaction consumes most of the oxygen in the combustion chamber. The oxygen that is needed for the combustion comes from the inlet only. The inlet design determines the amount of air entering the combustion chamber

and thus plays a significant role in valveless pulsejet performance.

ACKNOWLEDGEMENT

The authors are thankful to Dr. M. Venkata Ramana, Professor and Principal, Prof. K. Chandra Shekar, & Prof. S. Venugopal Rao for their constant encouragement and cooperation throughout the work.

REFERENCES

- [1] Rajput R.K., Thermal Engineering, 8th edition, Laxmi Publications
- [2] V. Ganesan - Ic Engines, Tata McGraw-Hill Education, 2002
- [3] I.A. Waitz, G. Gauba, Y. Tzeng, Fluids Eng. 120 (1998) pp 109–117.
- [4] C.M. Spadaccini, A. Mehra, J. Lee, X. Zhang, S. Lukachko, I.A. Waitz, Eng. Gas Turbines Power 125 (2003) pp 709–719.
- [5] G.D. Roy, S.M. Frolov, A.A. Borisov, D.W. Netzer, Prog. Energy Combust. Sci. 6 (2004) pp 545–672.
- [6] T. Geng, M.A. Schoen, A.V. Kuznetsov, W.L. Roberts, Flow Turbulence Combustion. Springer – vol 78, issue 1, pp 17-33
- [7] David Roylance, Finite Element Analysis Massachusetts Institute of Technology, Cambridge, USA, February 28, 2001. O.C. Zienkiewicz and R.L. Taylor, The Finite Element Method, McGraw-Hill Co., London, 1989